Reconstructions of Phase Contrast, Phased Array Multicoil Data

Matt A. Bernstein, Mladen Grgic, Thomas J. Brosnan, Norbert J. Pelc

We present a reconstruction method for phased array multicoil data that is compatible with phase contrast MR angiography. The proposed algorithm can produce either complex difference or phase difference angiograms. Directional flow and quantitative information are preserved with the phase difference reconstruction. The proposed method is computationally efficient and avoids intercoil cancellation errors near the velocity aliasing boundary. Feasibility of the method is demonstrated on human scans.

Key words: phase contrast; phased array; multicoil; reconstruction.

INTRODUCTION

Phase contrast (PC) angiography (1–8) can depict flow direction and volume rate, and also provide angiograms with excellent stationary tissue suppression. Like nearly all MRI techniques, however, phase contrast angiography has a limited signal-to-noise ratio (SNR), and must balance the requirements of imaging time, field of view, and resolution. The phased array (PA) technique (9–13) has demonstrated the SNR advantages of local surface coils, while retaining the fields of view of larger volume coils. The SNR of phase contrast images, reconstructed by either the complex difference or magnitude-masked phase difference method, is proportional to the SNR of the conventional magnitude reconstruction (7, 14). Thus, phased arrays can improve the SNR of phase contrast images as well.

PC-PA scans have been previously demonstrated by Swan *et al.* (15). That work used a standard PA magnitude reconstruction, in conjunction with the time-domain subtraction of the two PC flow acquisitions as described by Dumoulin *et al.* (5). Although that time domain subtraction produced high quality complex difference PC angiograms, it does not provide directional or quantitative flow information. The method described here provides that information, and is also compatible with image domain phase correction (16, M.A. Bernstein, N.J. Pelc, Phase correction of complex difference processed MR angiograms. U.S. Patent 5,226,418).

Reconstruction of phase images from PA data is complicated because each coil imparts its own location-dependent phase. These per-coil phases must be removed before reconstruction of the combined PA phase image. As will be shown, with phase *contrast* reconstructions, however, the phase subtraction step can conveniently remove the coil-dependent effects, thereby making joint PC-PA reconstructions easier.

The total amount of raw data produced by a PC-PA scan is larger than that of a single-coil magnitude scan by a factor equal to the product of the number coils and the number of flow acquisitions. Each of these factors can be four (or more) (5, 7, 9), so a combined PC-PA scan can typically generate 16 times the normal amount of raw data. This report describes a reconstruction algorithm developed with attention to computational efficiency, as required by such large amounts of data.

METHODS

Review of Phased Array Magnitude Reconstructions

First we review a simple, commonly used PA reconstruction (9, 10) for conventional magnitude images. Consider a phased array comprising $k = 1, 2, \ldots, N$ coils. The signal from coil k is separately digitized and stored as a set of complex numbers. The discrete Fourier transform of the data yields the single-coil complex image Z_k. The pixel-by-pixel modulus of Z_k provides the single-coil magnitude image, M_k.

The combined PA magnitude image is then given by:

$$M = \{\sum_k (M_k/\sigma_k)^2\}^{1/2} \quad [1]$$

where σ_k is the spatially independent noise estimate for the kth coil-preamplifier-receiver chain, measured during pre-scan calibration. The $\{\sigma_k\}$ are normalized so that $\Sigma 1/\sigma_k^2 = 1$.

Review of Phase Contrast Reconstructions

To obtain a vascular image representing flow along a single direction, subtraction is performed on a pair of flow acquisitions that have different gradient first moments along that direction. Two methods for performing this subtraction have been described most extensively in the literature: phase difference (2–4, 6–8) and complex difference (5).

Fourier transformation provides two complex images, Z_1 and Z_2. The phase difference $\Delta\Phi_x$ is calculated on a pixel-by-pixel basis:

$$-\pi \le \Delta\Phi_x = \arg(Z_1/Z_2) = \arg(Z_1 Z_2^*) \le \pi, \quad [2]$$

where * denotes complex conjugation, $\arg(A + iB) =$ arctangent (B/A), and we have assumed the gradient first moment in the x-direction was varied. The phase

MRM 32:330–334 (1994)

From GE Medical Systems, Waukesha, Wisconsin (M.A.B., M.G.); and Stanford University School of Medicine, Department of Radiology, Lucas MRS Imaging Center, Stanford, California (T.J.B., N.J.P.).

Address correspondence to: Matt Bernstein, Ph.D., W-875, Applied Science Laboratory, GE Medical Systems, 3200 N. Grandview Boulevard, Waukesha, WI 53188.

Received November 23, 1993; revised March 18, 1994; accepted May 10, 1994.

0740-3194/94 $3.00

difference $\Delta\Phi_x$ can then be phase corrected (16, M.A. Bernstein, N.J. Pelc, Phase correction of complex difference processed MR angiograms. U.S. Patent 5,226,418.), yielding $\Delta\Phi_{x(corr)}$, to account for background phase errors which arise mainly from gradient eddy currents.

Finally, a magnitude-mask can suppress the spurious phase values in regions of low signal (7):

magnitude masked phase image

$$= 0.5\,(M_1 + M_2)\,\Delta\Phi_{x(corr)}, \quad [3]$$

where $M_j = |Z_j|$. Alternatively, the complex difference reconstruction is:

$$CD_x = |Z_1 - Z_2|$$
$$= \{M_1^2 + M_2^2 - 2\,M_1\,M_2\cos(\Delta\Phi_{x(corr)})\}^{1/2} \quad [4]$$

Note the use of the law of cosines in Eq. [4] leads to explicit dependence on $\Delta\Phi_x$, so that the complex difference can be phase corrected.

An image depicting flow in all three directions (i.e., a "speed" image) can be formed with the complex difference method:

$$CD\text{speed} = \{(CD_x)^2 + (CD_y)^2 + (CD_z)^2\}^{1/2}, \quad [5]$$

or with the four-point (7, 8) phase difference method,

$$PD\text{speed} = \{0.25\,(M_1 + M_2 + M_3 + M_4)\,((\Delta\Phi_{x(corr)})^2 + (\Delta\Phi_{y(corr)})^2 + (\Delta\Phi_{z(corr)})^2)^{1/2}\}. \quad [6]$$

PC-PA Reconstruction Method

The PA combination is preferably performed after the PC phase subtraction so that the coil-dependent phases cancel. To minimize the reconstruction time, however, it is advantageous to perform the PA combination prior to as many processing steps as possible. Even with these guidelines, many alternative reconstruction methods are feasible. As described next, SNR considerations and inter-coil cancellation artifacts can help distinguish among them.

Consider the phase difference measured by coil k,

$$\phi_k = \arg\,(Z_{1k}\,Z_{2k}^*) \quad [7]$$

to be an estimate of the true velocity-induced phase difference $\Delta\Phi_x$. As long as the coils are uncoupled, the noise among $\{\phi_k\}$ are uncorrelated, but their variances are different due to spatial variations in SNR for each coil. The optimal combination of $\{\phi_k\}$ takes these variances into account. Assuming $M_{1k} = M_{2k}$, which is an excellent approximation for two-sided encoding (17), and letting $M_k = M_{1k} = M_{2k}$, the variance (7, 18) in ϕ_k is inversely proportional to M_k^2:

$$\text{var}(\phi_k) \propto 1/M_k^2. \quad [8]$$

The linear combination of $\{\phi_k\}$ that minimizes the variance of the combined result uses a weight for coil k that is inversely proportional to $\text{var}(\phi_k)$, i.e., magnitude-squared weighting. Thus, one estimate of true phase difference is:

$$\Delta\Phi_x = \Sigma\,M_k^2\,\phi_k/\Sigma M_k^2 \quad [9]$$

The method of Eq. [9], however, is subject to errors when the $\{\phi_k\}$ straddle the velocity aliasing boundary. A single-coil signed phase difference image can have discontinuities where the velocity is near the aliasing boundary. If Eq. [9] is used, however, then the discontinuities can also appear on speed and complex difference images. Further, Eq. [9] blurs the aliasing discontinuities, and precludes correction for aliasing. For example, in the simple case of $N = 2$ coils with $M_1 = M_2$, a true phase difference near π, $\phi_1 = \pi - \epsilon$, and $\phi_2 = -\pi + \epsilon$, then Eq. [9] yields the incorrect estimate $\Delta\Phi_x = 0$. This defect can be avoided by accumulating complex exponentials, rather than angles:

$$\arg\{\exp(i\,(\pi - \epsilon) + \exp(i\,(-\pi + \epsilon)\}$$
$$= \arg\{\exp\,(i\,\pi)\,2\cos(\epsilon)\} = \pi, \quad [10]$$

which is correct. The addition in Eq. [10] is illustrated by Fig. 1. (The pitfalls of working with angles rather than complex exponentials have been noted in the context of quantum mechanics by Peierls (19).)

Given the advantage of exponentials, one could ask which linear combination of $\{\exp(i\phi_k)\}$ minimizes the variance of the estimate of $\exp\,(i\Delta\Phi_x)$:

$$\text{var}(\exp(i\phi_k)) = [\partial\,\exp(i\phi_k)/\partial\,\phi_k]^2\,\text{var}(\phi_k) \propto 1/M_k^2. \quad [11]$$

Thus complex exponentials call for magnitude-squared weighting as well. We can exploit the intrinsic magnitude-squared scaling in the terms

$$Z_{1k}\,Z_{2k}^* = M_{1k}\,M_{2k}\exp(i\phi_k) \quad [12]$$

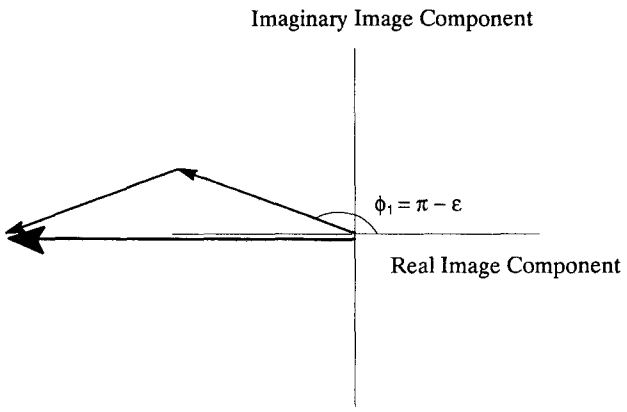

FIG. 1. A pitfall of estimating the combined phased array velocity-induced phase difference by adding angles instead of complex exponentials. The two short arrows each represent the magnitude-squared weighted complex exponentials for a single coil, as calculated by Eq. [12]. The flow-induced phase difference is indicated by the angle between the arrow and the real axis. Suppose the individual phase differences measured with a two-coil array are $\phi_1 = \pi - \epsilon$, and $\phi_2 = -\pi + \epsilon$, and the magnitudes are equal, $M_1 = M_2$. Simply taking a weighted average of the angles leads to the incorrect estimate of $\Delta\Phi_x = 0$. But adding weighted complex exponentials, as shown, yields the correct estimate of $\Delta\Phi_x = \pi$.

to form the estimate of $\exp(i\Delta\Phi_x)$. Including the measured coil-dependent noise factors σ_k, the estimate for the phase difference becomes:

$$\Delta\Phi_x = \arg\{\sum_k Z_{1k} Z_{2k}^*/\sigma_k^2\}, \quad [13]$$

and similarly for $\Delta\Phi_y$, and $\Delta\Phi_z$. The physical significance of this magnitude squared weighting is depicted by Fig. 2. Equation [13] is computationally efficient because only one arctangent and one phase correction operation per flow direction are required, regardless of the number of coils. Additionally, if geometrical correction is required for gradient nonuniformities, it need only be done once per scan location. The magnitude images called for by Eqs. [3], [4], and [6] can be reconstructed with the conventional PA reconstruction given by Eq. [1]. Alternatively, the average magnitude image of Eq. [3] can be estimated from

$$M_{ave} = |\{\sum_k Z_{1k} Z_{2k}^*/\sigma_k^2\}|^{1/2}, \quad [14]$$

Equation [13] is the central result of the proposed method. At this stage the PA combination is complete, and the combined phase difference calculated by Eq. [13] may be substituted into Eqs. [3], [4], and [6] as desired.

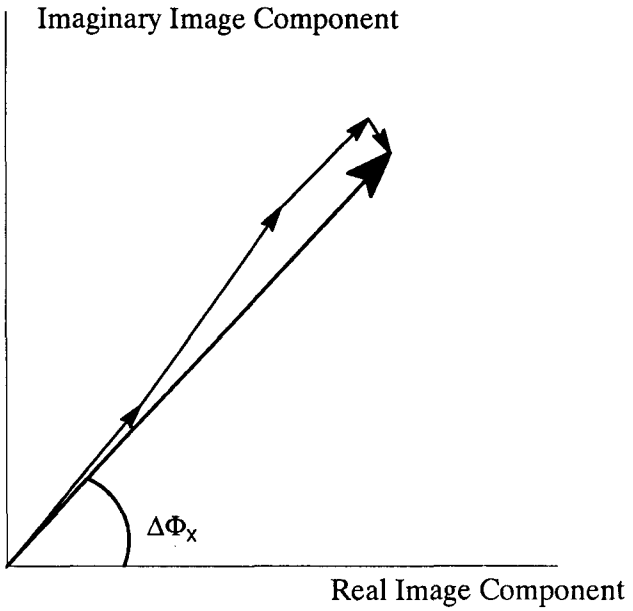

FIG. 2. The combined phased array phase difference $\Delta\Phi_x$ is estimated from phases measured with individual coils. The *k*th arrow represents the magnitude-squared weighted complex exponential $Z_{1k} Z_{2k}$. Suppose one coil produces a relatively weak signal (depicted by the short arrow). Typically the phase difference measured by that coil will be inaccurate since, according to Eq. [8], its variance large. The intrinsic magnitude-squared weighting in Eq. [13] assures that those coils with the weak signal contribute proportionately less to the estimate or $\Delta\Phi_x$.

RESULTS

We implemented the described method on a 1.5 T scanner (Signa with level 5.4 software, GE Medical Systems, Milwaukee, WI) equipped with an i860 array processor (Mercury Computer Systems, Inc, Chelmsford, MA). With this system, a single-coil 256 × 256 single-direction phase difference image reconstructs in 2.6 s, including transfer time to the image processor. Using Eqs. [1], [3], and [13], the equivalent four-coil image reconstruction takes 6.3 s. Because the ratio of reconstruction times is less than four, we consider the proposed method "efficient."

We measured volume flow rates in a phantom using the phase difference reconstruction with both the cervical-thoracic-lumbar (CTL) phased array and the body coil. A model 2630 pump (Cole Palmer Instrument Co, Niles, IL) provided flow through a 1-cm inside diameter Tygon tube, which was constant over time to better than 1% as measured by an FM2000C digital flow meter (Stellar Instruments, Irvine, CA.). The body coil scan used the same reconstruction that previously has been validated for flow quantification (6). Data were acquired with two flow tubes at 16 cardiac phases, each scanned at two axial locations where two of the four coils contributed approximately equal signal to the PA-combined image. (Because the flow rate was constant, multiple "cardiac phases" were used to provide more statistical data, rather than provide temporal resolution.) Flow rate was measured in each frame, and the mean and standard deviation of the 64 flow measurements (16 frames × 2 tubes × 2 locations) were computed. The volume flow rate measured with the CTL coil and PC-PA reconstruction was 1447 ± 20 ml/min; the body coil measurement yielded 1442 ± 29 ml/min. The flow, as measured by timing the filling of a graduated cylinder, was 1490 ± 44 ml/min. The observed accuracy is in line with expectations considering the known sources of systematic errors in phase contrast flow measurements, particularly those arising from region of interest definition (20). (The area measurement needed to convert from velocity to volume flow rate was determined by the 50% level on the corresponding magnitude images, with no further partial volume correction.) The data suggest to us that the PC-PA reconstruction can be used to quantify flow.

Phase difference images of a normal volunteer were acquired with the body coil as well as with a pelvic phased array receive coil, and reconstructed as described in Methods. The acquisition parameters were TR = 26 ms, TE = 9.2 ms, aliasing velocity VENC = 100 cm/s, flow sensitivity in the superior-inferior direction, 256 × 192 matrix, 24 × 24 cm field of view, 5 mm thick, retrospectively gated cine acquisition, and 1 signal average yielding an acquisition time of 192 heartbeats (4 min 30 s). Figure 3 (left) represents a single cardiac phase from a total of 16 reconstructed phases acquired with the body coil. Magnitude (top) and magnitude-masked phase difference (bottom) images are shown. This axial section was positioned in the abdomen inferior to the aortic bifurcation. Figure 3 (right) shows the equivalent images from the phased array coil, reconstructed with Eq. [13]. The phased array image demonstrates a lower noise floor, providing greater detectability of small vessels. The SNR

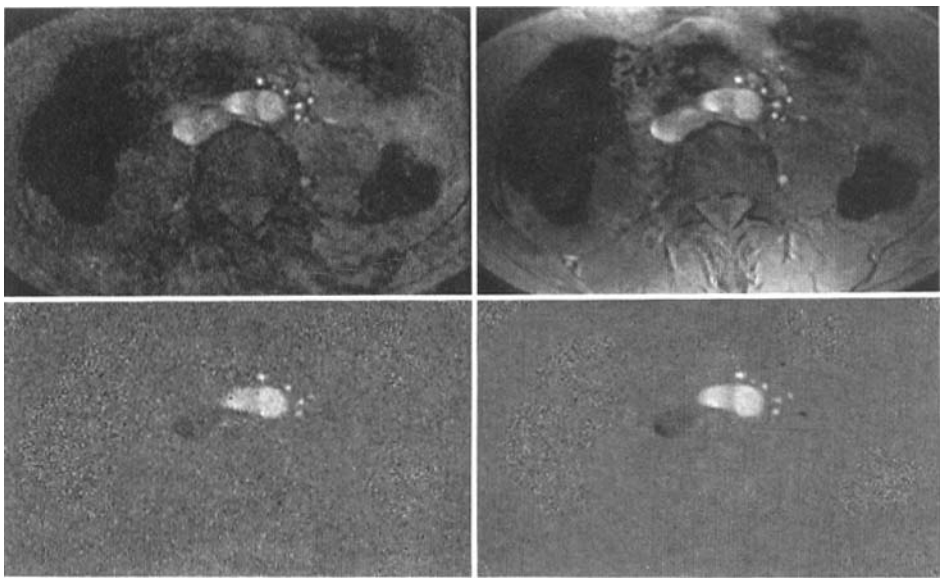

FIG. 3. Phase contrast scans of a normal volunteer reconstructed with the phase difference method. A single cardiac phase from 16 retrospectively gated phases is shown. Top: magnitude images, bottom: magnitude-masked phase difference images. Left: body coil as reconstruction with Eq. [3], right: pelvic phased array, as reconstructed with Eqs. [3] and [13].

measured in the left main vessel is 6.7 with the body coil, and 10.1 with the phased array.

Figure 4a shows a complex difference image acquired with the body coil. The acquisition parameters were TR = 33 ms, TE = 9.4 ms, aliasing velocity VENC = 40 cm/s, 4-set acquisition sensitive to flow in all directions, 512 × 256 matrix providing a 32 × 16 cm field of view, a single 70-mm thick slab, and eight signal averages for an acquisition time of 2 min 17 s. The same parameters were used for an acquisition with a phased array coil, composed of an anterior neck coil, and three 5-inch coils positioned right, left, and anterior to the head (Fig. 4b). The improved SNR of the phased array image is apparent. The transmit-receive quadrature head coil produced SNR comparable to that of Fig. 4b, but with only approximately 2/3 the superior-inferior coverage.

Although Figs. 3 and 4 demonstrate that phased array can improve the SNR of phase contrast images, careful coil selection is necessary to produce good results. For example, if one of the coils in the phased array is placed near moving tissue, which produces an intense signal, the imperfect phase subtraction from that coil can degrade the image. We observed this effect with a supine patient and a coil placed near the anterior abdominal wall, which moves with respiration. By removing the two anterior coils, a two-coil array produced images of the renal arteries which were superior to those from the four-coil array. Another point to consider is a reduced noise floor, which implies a greater artifact-to-noise ratio, and possibly more conspicuous ghosting artifacts.

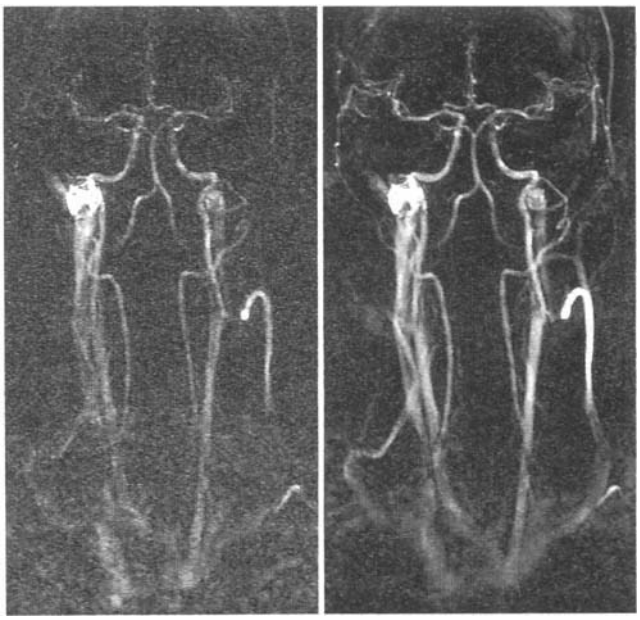

FIG. 4. Phase contrast angiograms of a normal volunteer processed with the complex difference reconstruction. The images were obtained with a) the body coil, as reconstructed with Eqs. [4] and [5]. b) A four-coil phased array as reconstructed with Eqs. [4], [5], and [13]. Each scan was obtained in 2 min 17 s. See text.

SUMMARY

A phase contrast reconstruction method that is compatible with phased array multicoil acquisitions has been presented. The method is relatively computationally efficient in that a four-coil reconstruction takes only about 2.4 times as long as a single coil reconstruction. The computational efficiency is achieved by employing only single arctangent and phase correction operations per flow direction, regardless of the number of coils. (Geometrical distortion may be corrected after the PA combination on a per-location basis.) The method estimates the combined velocity-induced phase difference with magnitude-squared weighting of the individual coil measurements for SNR considerations. Also the method accumulates complex exponentials, rather than angles, for immunity to intercoil phase cancellation when the phases straddle the $\pm\pi$ boundary. The feasibility of the method was demonstrated with scans of a flow phantom and normal volunteers.

ACKNOWLEDGMENTS

The authors thank R. Scott Hinks for use of his flow phantom, J. Douglas Martin for assistance with the flow phantom measurements, and Bruce Collick for useful discussions on magnitude phased array reconstructions.

REFERENCES

1. P. R. Moran, A flow velocity zeumatographic interlace for NMR imaging in humans. *Magn. Reson. Imaging* **1,** 197–203 (1982).
2. D. J. Bryant, J. A. Payne, D. N. Firmin, D. B. Longmore, Measurement of flow with NMR imaging using a gradient pulse and phase difference technique. *J. Comput. Assist. Tomogr.* **8,** 588–593 (1984).
3. M. O'Donnell, NMR blood flow imaging using multiecho, phase contrast sequences. *Med. Phys.* **12,** 59–64 (1985).
4. G. L. Nayler, D. N. Firmin, D. B. Longmore, Blood flow imaging by cine magnetic resonance. *J. Comput. Assist. Tomogr.* **10,** 715–722 (1986).
5. C. L. Dumoulin, S. P. Souza, M. F. Walker, W. Wagle, Three-dimensional phase contrast angiography. *Magn. Reson. Med.* **9,** 139–149 (1989).
6. C. E. Spritzer, N. J. Pelc, J. N. Lee, A. J. Evans, H. D. Sostman, S. J. Riederer, Rapid MR imaging of blood flow with a phase-sensitive, limited-flip-angle, gradient recalled pulse sequence: preliminary experience. *Radiology* **176,** 255–262 (1990).
7. N. J. Pelc, M. A. Bernstein, A. Shimakawa, G. H. Glover, Encoding strategies for three-direction phase contrast MR imaging of flow. *J. Magn. Reson. Imaging* **1,** 405–413 (1991).
8. R. Haussmann, J. S. Lewin, G. Laub, Phase-contrast MR angiography with reduced acquisition time: new concepts in sequence design. *J. Magn. Reson. Imaging* **1,** 415–422 (1991).
9. P. B. Roemer, W. A. Edelstein, C. E. Hayes, S. P. Souza, O. M. Mueller, The NMR phased array. *Magn. Reson. Med.* **16,** 192–225 (1990).
10. C. E. Hayes, P. B. Roemer, Noise correlations in data simultaneously acquired from multiple surface coil arrays. *Magn. Reson. Med.* **16,** 181–191 (1990).
11. C. E. Hayes, N. Hattes, P. B. Roemer, Volume imaging with MR phased arrays. *Magn. Reson. Med.* **18,** 309–319 (1991).
12. R. C. Smith, C. Reinhold, T. R. McCauley, R. C. Lange, R. T. Constable, R. Kier, S. McCarthy, Multicoil high-resolution fast spin-echo imaging of the female pelvis. *Radiology* **184,** 671–675 (1992).
13. C. E. Hayes, M. J. Dietz, B. F. King, R. L. Ehman, Pelvic imaging with phased array coils: quantitative assessment of SNR improvement. *J. Magn. Reson. Imaging* **2,** 321–326 (1992).
14. M. A. Bernstein, Y. Ikezaki, Comparison of phase-difference and complex-difference processing in phase-contrast MR angiography. *J. Magn. Reson. Imaging* **1,** 725–729 (1991).
15. J. S. Swan, T. M. Grist, D. M. Weber, I. Sproat, M. M. Wojtowycz, MR angiography of the pelvis with variable velocity encoding and a phased-array coil. *Radiology* **190,** 363–370 (1994).
16. J. J. E. In den Kleef, J. P. Groen, A spatially non-linear phase correction for MR angiography, *in* "Proc., SMRM, 6th Annual Meeting, 1987," p. 29.
17. M. A. Bernstein, A. Shimakawa, N. J. Pelc, Minimizing *TE* in moment-nulled or flow encoded two- and three-dimensional gradient echo imaging. *J. Magn. Reson. Imaging* **2,** 583–588 (1992).
18. T. E. Conturo, G. D. Smith, Signal-to-noise in phase angle reconstruction: dynamic range extension using phase reference offsets. *Magn. Reson. Med.* **15,** 420–437 (1990).
19. R. E. Peierls, "Surprises in Theoretical Physics," section 1.4, Princeton University Press, Princeton, NJ, 1979.
20. C. Tang, D. D. Blatter, D. L. Parker, Accuracy of phase-contrast flow measurements in the presence of partial-volume effects. *J. Magn. Reson. Imaging* **3,** 377–385 (1993).